Pergamon

Int. J. Solids Structures Vol. 33, No. 1, pp. 19–31, 1996

0020-7683/96 $9.50 + .00

0020-7683(95)00024-0

PLANAR FORCING OF FLOATING ICE SHEETS

Z. G. ZHAO and J. P. DEMPSEY
Department of Civil and Environmental Engineering, Clarkson University, Potsdam, NY 13699-5710, U.S.A.

(*Received* 12 *August* 1994; *in revised form* 3 *January* 1995)

Abstract—The objective of this study is to investigate the plane dynamic response of a floating plate supported by a fluid. The fluid underneath the plate is modeled using two-dimensional incompressible potential flow theory. The fundamental solutions are obtained first. Once the solution for the plate displacement is obtained, the other physical quantities of interest—the temporal and spatial distributions of the slope, moment, shear and even the buoyant force, the inertial force of the fluid and the inertial force of the plate—can be evaluated numerically. Advantageously, using superposition and the fundamental solutions presented in this paper, the solution for various loading cases can be readily obtained. As an application, the dynamic behavior of a forced sub-surface uplift problem is studied. Comparisons are then made with an added mass model. The results reveal that the true hydrodynamic model increases the mass and damping of the plate significantly.

1. INTRODUCTION

In this study, the plane dynamic response of an infinite plate is considered (Fig. 1). The floating plate may represent, for instance, an ice sheet, in which case it is infinite in both directions of the plane (x and y); the external loading is considered to be uniformly distributed in the y direction. One practical use for the class of solution developed in this paper is the sudden loading of ice sheets; obvious examples include submarine surfacings and aircraft landings. Elastostatic layer studies (Dempsey *et al.*, 1990) reveal that elastic plate theory can predict accurate results as long as the ratio of the characteristic length [see eqn (4)] over the layer thickness is larger than eight. The fluid underneath the plate is modeled using two-dimensional incompressible potential flow theory. Using Fourier transforms, the fluid–plate interface pressure is expressed in terms of the transformed plate deflection and its derivative; the governing equation reduces to an ordinary differential equation. Ultimately, the deflection of the plate is expressed in terms of an integral of the surface loading.

Sodhi (1989) recently conducted a series of small-scale tests for submarine surfacing under given motion of the indenter, in which the floating model ice sheets were pushed vertically upwards by cylindrical indenters. When the dimension of the indenter in one direction is much larger than that in other direction, the problem can be treated as a planar forced uplift. Using fundamental solutions presented in this paper, the problem is reduced to a Volterra integral equation of the first kind. Volterra integral equations of the first kind are difficult to treat. After some numerical experimentation, it proved advantageous to transform the governing equation into an integro-differential equation.

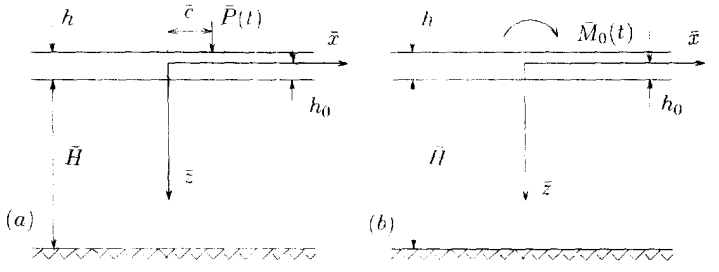

Fig. 1. Problem configuration and coordinates: (a) a concentrated force; (b) a concentrated moment on a floating plate.

2. PROBLEM DESCRIPTION

The fluid under the plate is modeled using two-dimensional incompressible potential flow theory. The motion of the floating plate is modeled using Euler–Bernoulli plate theory:

$$c_a B\rho_i h\frac{\partial^2\bar{w}}{\partial t^2}+E'I\frac{\partial^4\bar{w}}{\partial\bar{x}^4}+\bar{p}_0=\bar{q}(\bar{x},t)-N\frac{\partial^2\bar{w}}{\partial\bar{x}^2}, \tag{1}$$

where $E'I$ is the flexural rigidity of the plate, ρ_i is its mass density, h the vertical thickness, B the width, $\bar{w}$ the vertical displacement and $\bar{q}(\bar{x},t)$ is the surface loading on the plate. In eqn (1), $c_a=1$ for the elastohydrodynamic model; for the added mass model, c_a is unknown at present (and is to be determined); $\bar{p}_0$ is the fluid–plate interface pressure exerted by the hydrodynamic reaction. In the last term of eqn (1), $N=\bar{\sigma}h$ is the in-plane compressive force, where $\bar{\sigma}$ is the in-plane (thermal or residual) stress in the plate. For sea ice sheets, $\bar{\sigma}$ may vary between -300 kPa and 0.

Non-dimensional quantities and coordinates, as well as the Fourier transform with respect to x, are introduced for the governing equation and the associated boundary and initial conditions,

$$(z,w)=(\bar{z},\bar{w})/h,\quad (H,x,c)=(\bar{H},\bar{x},\bar{c})/l; \tag{2a}$$

$$(p_0,q)=(\bar{p}_0,\bar{q})/\rho_w gh,\quad \mu=\rho_i h/\rho_w l,\quad \phi=\bar{\phi}/[h\sqrt{(gl)}]; \tag{2b}$$

$$\tau=t\sqrt{(g/l)},P(\tau)=\bar{P}(t)/\rho_w gBlh,\quad \sigma=N/\rho_w gl^2, \tag{2c}$$

$$\mathcal{F}\{f\}=F(\gamma,\tau)=\frac{1}{2\pi}\int_{-\infty}^{\infty}f(x,\tau)\,e^{i\gamma x}\,dx, \tag{3a}$$

$$\mathcal{F}^{-1}\{F\}=f(x,\tau)=\int_{-\infty}^{\infty}F(\gamma,\tau)\,e^{-i\gamma x}\,d\gamma. \tag{3b}$$

In eqn (2),

$$l=(E'I/\rho_w g)^{1/4} \tag{4}$$

denotes the characteristic length. For an isotropic, homogeneous elastic plate, $E'=E/(1-\nu^2)$ for plane strain ($B=1$) while $E'=E$ for plane stress.

The bottom-surface pressure due to the acceleration of the water is treated by assuming that the motion of the water is governed by two-dimensional potential flow theory (Kheisin, 1967; Nevel, 1970; Dempsey and Zhao, 1993). This interface pressure also acts in the contact area. To this end, let ϕ be the corresponding water potential function; assuming that the water is incompressible and irrotational, conservation of water mass requires that

$$\nabla^2\phi=\frac{\partial^2\phi}{\partial x^2}+\left(\frac{h}{l}\right)^2\frac{\partial^2\phi}{\partial z^2}=0. \tag{5}$$

The water velocity vector $\mathbf{v}$ is the gradient of the potential function ϕ. At the deformed fluid water interface $z_i=\bar{w}+h_0$, the vertical velocity of the fluid is equal to the vertical velocity of the plate. Assuming that the depth $\bar{H}$ of the fluid under the plate is a constant, the vertical velocity at $z=(\bar{H}+h_0)$ is zero. Physically, as x approaches infinity, the velocity is zero. Therefore, ϕ approaches to a constant, and it is set equal to zero as x approaches infinity. The boundary conditions on the fluid layer (Dempsey and Zhao, 1993) are then given by

$$\left.\frac{\partial \phi}{\partial z}\right|_{z=h_0 h} = \frac{h}{l}\frac{\partial w}{\partial \tau}, \tag{6a}$$

$$\left.\frac{\partial \phi}{\partial z}\right|_{z=H+h_0 h} = 0, \tag{6b}$$

$$\phi|_{x\to\infty} = 0. \tag{6c}$$

The pressure p_0 in eqn (3) may then be determined from Bernoulli's equation, assuming that the water has no viscosity and that as x approaches infinity, $\mathbf{v}\cdot\mathbf{v} = 0$, $p_0 = 0$ and $w = 0$,

$$p_0 = w - c_h \left.\frac{\partial \phi}{\partial \tau}\right|_{z=h_0 h}, \tag{7}$$

in which the term proportional to the square of the vertical velocity is omitted because of its non-linearity and the influence of this term on the results is not significant; $c_h = 0$ for the added mass model, while $c_h = 1$ for the elastohydrodynamic model. No material damping is included.

The motion of the floating plate in non-dimensional form is given by

$$c_a \mu \frac{\partial^2 w}{\partial \tau^2} - c_h \left.\frac{\partial \phi}{\partial \tau}\right|_{z=h_0 h} + \frac{\partial^4 w}{\partial x^4} + w = q(x,\tau) - \sigma \frac{\partial^2 w}{\partial x^2}. \tag{8}$$

Using Fourier transforms, eqn (5) for the transformed potential function, which is used in evaluating the transformed pressure from eqn (7), is reduced to

$$\mathscr{F}\{\nabla^2 \phi\} = \frac{\partial^2 \Phi}{\partial z^2} - (\gamma h/l)^2 \Phi = 0. \tag{9}$$

Therefore, the condition in eqn (6) requires that (using $\bar{\gamma} = \gamma h/l$)

$$\Phi = A_1 \cosh(\bar{\gamma} z) + A_2 \sinh(\bar{\gamma} z). \tag{10}$$

The constants A_1 and A_2 are determined by using transform of boundary conditions (6a,b). Eventually, the Fourier transform of eqn (7) becomes,

$$\mathscr{P}_0 = \mathscr{F}\{p_0\} = W + c_h \frac{\partial^2 W}{\partial \tau^2} \frac{1}{\gamma \tanh \gamma H}. \tag{11}$$

3. FUNDAMENTAL SOLUTIONS

When the floating plate is subjected to a concentrated load at $\bar{x} = \bar{c}$ [Fig. 1(a)],

$$\bar{q}(\bar{x}, t) = \bar{P}_0 f^*(t) \delta(\bar{x} - \bar{c})\, B, \tag{12}$$

where $\delta(\cdot)$ is a delta function, $\bar{P}_0 = \rho_w g B l h P_0$ is the value of the applied load and the time function $f^*(t) = f(\tau)$ indicates the variation of the external force with time. Substituting eqn (12) and the non-dimensional notation in (2) into eqn (8), the Fourier transform of eqn (8) gives

$$\left(c_a\mu+\frac{c_h}{\gamma\tanh\gamma H}\right)\frac{\partial^2 W}{\partial\tau^2}+(1+\sigma\gamma^2+\gamma^4)W=\frac{P_0}{2\pi}f(\tau)\,e^{i\gamma x}. \tag{13}$$

The solution for the transformed deflection $W(\gamma,\tau)$ is readily obtained as

$$W(\gamma,\tau)=\frac{P_0}{2\pi}\frac{\beta_\gamma e^{i\gamma x}}{1+\sigma\gamma^2+\gamma^4}I(\beta_\gamma,\tau), \tag{14}$$

in which

$$I(\beta_\gamma,\tau)=\int_0^\tau f(u)\sin[\beta_\gamma(\tau-u)]\,du, \tag{15}$$

is the convolution of the time function $f(\tau)$, and

$$\beta_\gamma^2=\frac{1+\sigma\gamma^2+\gamma^4}{\mu_\gamma},\quad \mu_\gamma=c_a\mu+\frac{c_h}{\gamma\tanh(\gamma H)}. \tag{16}$$

For later use, note that if $f(\tau)$ is the Heaviside function, $I(\beta_\gamma,\tau)=(1-\cos\beta_\gamma\tau)/\beta_\gamma$. The displacement of the plate is quickly obtained by the inverse transform (3b). Noting that the function inside the integral is even in γ,

$$w(x,\tau)=\frac{P_0}{\pi}\int_0^\infty\frac{\beta_\gamma\cos[\gamma(x-c)]}{1+\sigma\gamma^2+\gamma^4}I(\beta_\gamma,\tau)\,d\gamma. \tag{17a}$$

The slope, moment and shear force can readily be written as

$$\theta(x,\tau)=\frac{\tilde\theta(\bar x,t)l}{h}=-\frac{P_0}{\pi}\int_0^\infty\frac{\beta_\gamma\gamma\sin[\gamma(x-c)]}{1+\sigma\gamma^2+\gamma^4}I(\beta_\gamma,\tau)\,d\gamma, \tag{17b}$$

$$M(x,\tau)=\frac{\tilde M(\bar x,t)l^2}{BhE'I}=-\frac{P_0}{\pi}\int_0^\infty\frac{\beta_\gamma\gamma^2\cos[\gamma(x-c)]}{1+\sigma\gamma^2+\gamma^4}I(\beta_\gamma,\tau)\,d\gamma, \tag{17c}$$

$$Q(x,\tau)=\frac{\tilde Q(\bar x,t)l^3}{BhE'I}=-\frac{P_0}{\pi}\int_0^\infty\frac{\beta_\gamma\gamma^3\sin[\gamma(x-c)]}{1+\sigma\gamma^2+\gamma^4}I(\beta_\gamma,\tau)\,d\gamma. \tag{17d}$$

These are the Green's functions of the title problem. For the symmetric loading, $\bar q(\bar x,t)=\bar P_0 f^*(t)[\delta(\bar x-\bar c)+\delta(\bar x+\bar c)]/2B$, the solution can be obtained by using eqn (17) and superposition

$$w(x,\tau)=\frac{P_0}{\pi}\int_0^\infty\frac{\beta_\gamma\cos(\gamma c)\cos(\gamma x)}{1+\sigma\gamma^2+\gamma^4}I(\beta_\gamma,\tau)\,d\gamma. \tag{18}$$

For the antisymmetric loading, $\bar q(\bar x,t)=\bar P_0 f^*(t)[\delta(\bar x-\bar c)-\delta(\bar x+\bar c)]/2B$, similarly, the solution can be obtained

$$w(x,\tau)=\frac{P_0}{\pi}\int_0^\infty\frac{\beta_\gamma\sin(\gamma c)\sin(\gamma x)}{1+\sigma\gamma^2+\gamma^4}I(\beta_\gamma,\tau)\,d\gamma. \tag{19}$$

Defining $\bar M_0=\bar P_0\bar c$ as a finite value, when $\bar c\to 0$, $\sin(\gamma c)/\gamma c\to 1$, and letting

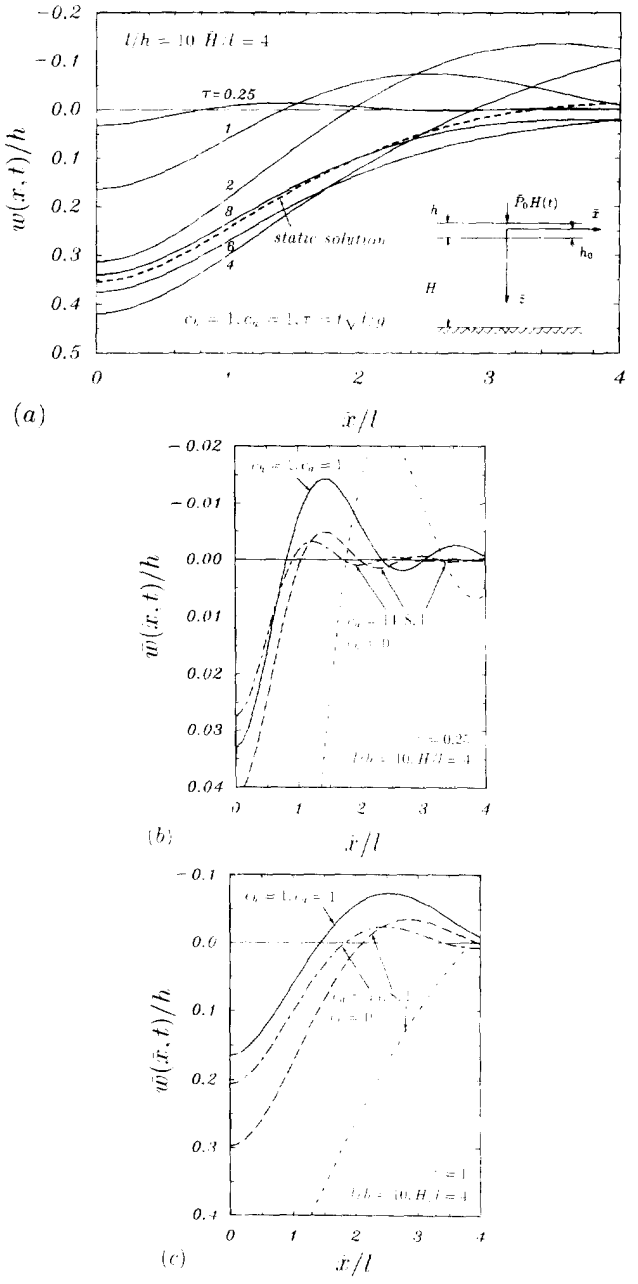

Fig. 2. Displacement of a floating plate subjected to a sudden force: (a) hydrodynamic solution; (b) hydrodynamic vs added mass model at $\tau = 0.25$ and (c) at $\tau = 1.0$.

$M_0 = \bar{M}_0/(\rho_w g l^2 h B) = \bar{M}_0/(BhEI)$, eqn (19) leads to the solution for a concentrated moment [Fig. 1(b)],

$$w(x,\tau) = \frac{M_0}{\pi} \int_0^\infty \frac{\beta \gamma \sin(\gamma x)}{1 + \sigma_0 \gamma^2 + \gamma^4} I(\beta, \tau)\, d\gamma. \tag{20}$$

Using the fundamental solutions (17), (20) and superposition, the solution for various loading cases can be readily obtained. In these evaluations, the in-plane stress σ_0 is assumed to be zero. The influence of the in-plane stress on the dynamic response will be discussed in the dynamic forced uplift problem.

The deflection of a floating plate subjected to a sudden concentrated load $\bar{P}_0 H(t)$ at the origin is portrayed in Fig. 2. Figure 2(a) shows that the difference between the static

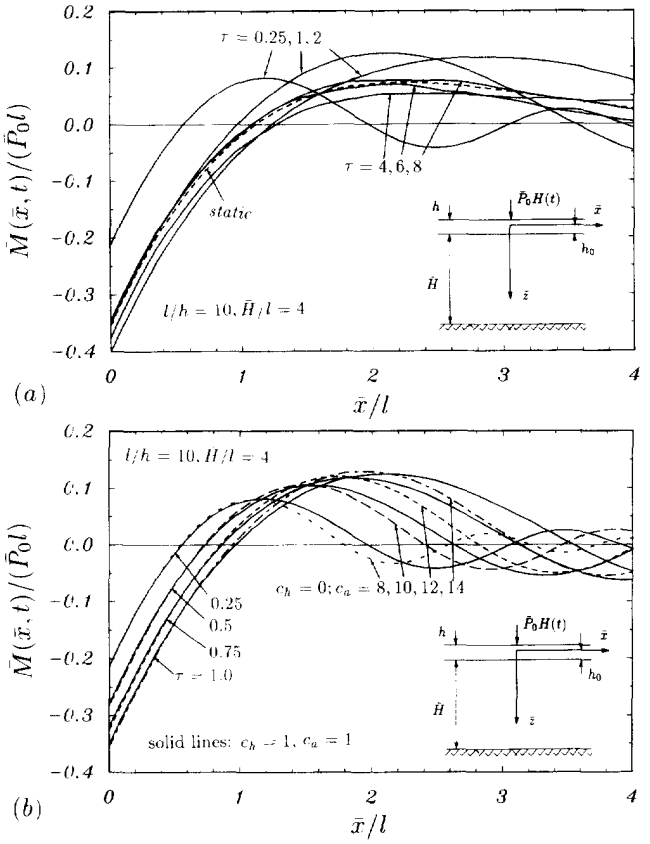

Fig. 3. Moment distribution of a floating plate subjected to a sudden force: (a) hydrodynamic solution; (b) hydrodynamic vs added mass solutions.

solution (Timoshenko, 1958) and the dynamic solution is pronounced for early times but is much reduced for later times. The hydrodynamic coupling decreases the rate of change of the displacement in the vicinity of the load but dramatically increases the above- and below-surface deflections away from the load. This feature reflects the volume conservation in the fluid layer, implicit in the incompressible and irrotational flow theory used. Figures 2(b, c) compare the hydrodynamic solution ($c_a = 1$, $c_h = 1$) with the added mass model ($c_h = 0$) for an early and later time. The added mass model ($c_h = 0$) can be constructed to fit the hydrodynamic solution for a chosen range of $\bar{x}/l$ and for early or later times; however, different c_a values are required for each specific case. The complexity of the elastohydrodynamic coupling is clearly not readily treated by an added mass model of the type chosen in this paper.

The moment distribution for a floating plate subjected to a sudden concentrated load $\bar{P}_0 H(t)$ at the origin is plotted in Fig. 3. Figure 3(a) reveals the similarity between the static solution and the hydrodynamic solution. Only for early times does the moment distribution differ markedly. Figure 3(b) compares the hydrodynamic and added mass models for various normalized times τ [$t = \tau\sqrt{(l/g)}$]. These particular moment distributions have been fitted for the initial range of $\bar{x}/l(|\bar{x}| \leqslant 1.5l)$ by choosing the optimum added mass coefficient. The range of the added mass is 7–13 times the mass of the plate for $\tau \leqslant 1.0$, and increases as time increases. The added mass model can accurately predict the bending moment near the loading area by choosing suitable coefficients c_a. The far-field moments are substantially underpredicted by the added mass model. Another feature of the moment distribution is that the moment from the added mass model oscillates more than that from hydrodynamic model. The obvious effect of the fluid inertia on the plate is to increase the mass and the damping of the plate significantly. While an increasing added mass coefficient is required for later times, it should be noted that the agreement between the moment distributions is

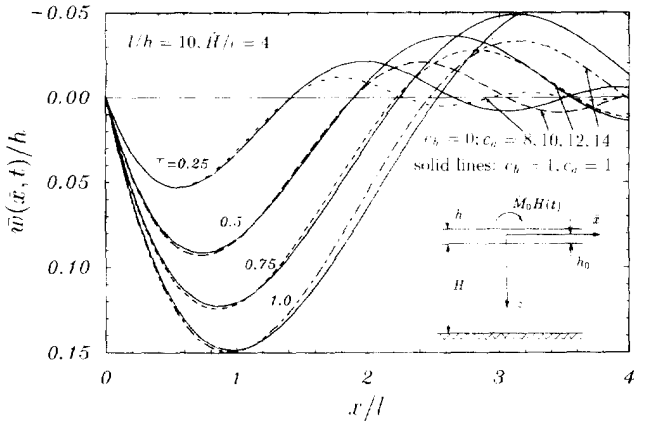

Fig. 4. Displacement of a floating plate subjected to a sudden moment: hydrodynamic vs added mass solutions.

much better than for the deflections. The moment does not rapidly redistribute with time; in addition, the moment is maximum under the load for the times considered.

The deflection induced by a sudden concentrated moment $\bar{M}_0H(t)$ at the origin is plotted in Fig. 4. The solid lines represent the solution of hydrodynamic model while the dashed lines indicate the solution of the added mass model. The deflection is zero at $\bar{x}/l = 0$ since the load is antisymmetric. Trial and error is used to find the best agreement near the loading area ($\bar{x}/l \leqslant 2$). Similar to Fig. 3(b), the far-field displacements are substantially underpredicted by the added mass model. The range of the added mass is 7–13 times the mass of the plate for $\tau \leqslant 1.0$, and increases as time increases. The maximum deflection occurs near $\bar{x}/l = 0.6$ for $\tau = 0.25$ and $\bar{x}/l = 1$ for $\tau = 1$.

The moment distribution for a floating plate subjected to a concentrated moment is plotted in Fig. 5. Figures 5(a,b) compare the normalized hydrodynamic solution with specific added mass solutions, evaluated at $\tau = 0.25$ and $\tau = 1.0$, respectively. The coefficients $c_a = 8$ and 14 for the added mass model are presented. Clearly, for early times, near the loading area ($\bar{x}/l \leqslant 1.0$), the added mass model is satisfactory while for the far-field, the moments are significantly different from the added mass solution. Again, the added mass moment distribution oscillates faster than that of the hydrodynamic model. For later times, when the hydrodynamic effects are not as pronounced, the added mass concept is more effective.

4. DYNAMIC FORCED UPLIFT

In the forced uplift problem (Fig. 6), the plate is assumed to be at rest before contact while the indenter moves upwards at a constant velocity v_0. During the early stages of contact, the indenter has some deceleration but quickly returns to its velocity v_0; meanwhile, the plate experiences acceleration in and close to the contact region and in the contact zone attains the velocity v_0 very quickly. In this paper, the approach is to describe effectively the uplift motion and then determine the necessary uplift force to accomplish this prescribed motion. The uplift of the floating plate by the indenter is thus described as

$$\bar{w}(0,t) = -h[v_0 t/h - (1 - e^{-v_0 t/h})\alpha], \tag{21}$$

where the parameter α is a function of the geometry of the indenter, and the amount of crushing between the indenter and the plate. The "best" value for α is influenced also by the fluid flow occurring prior to contact and any inelastic processes (cracking, creep) that occur during uplift. This parameter needs to be determined by comparisons with experiments; the advantage of the expression stated in eqn (21) is the resulting problem simplification and the ability to evaluate the influences of plate thickness and indenter velocity on the uplift force. The normalized uplift motion of the indenter in eqn (21) is

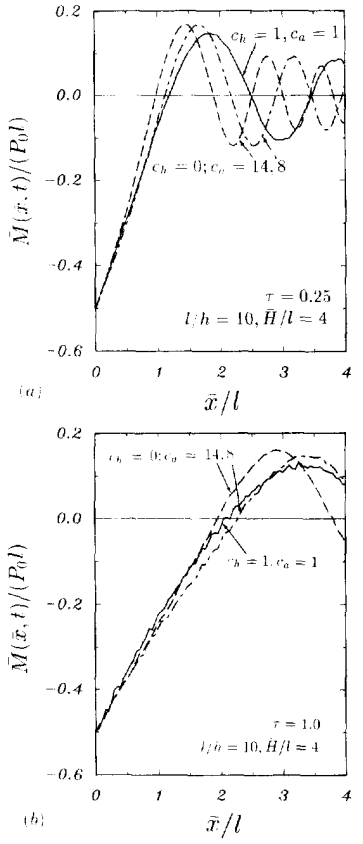

Fig. 5. Moment distribution in a floating plate subjected to a sudden moment: (a) hydrodynamic vs added mass model at $\tau = 0.25$ and (b) at $\tau = 1.0$.

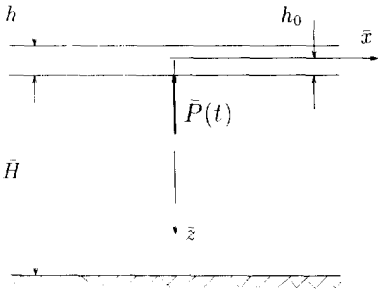

Fig. 6. Coordinates and loading configuration: forced planar uplift.

$$w(0,\tau) = -[\tilde{t} - (1 - e^{-\alpha \tilde{t}})/\alpha], \tag{22}$$

in which $\tilde{t} = \tau(v_\infty/h)\sqrt{(l/g)}$.

The indentation time constant h/v_∞ is of course the time taken by the indenter to traverse the plate thickness if no deceleration on contact were to take place. The ratio h/v_∞ is used as a time normalization parameter in eqn (21) and for the solutions obtained in this paper. The assumptions of small deformations and negligible creep effects necessarily restrict the solutions to times $v_\infty/h < 0.2$.

The uplift load required is an unknown time function and is to be determined. Assuming the indenter is a long rigid strip, the distribution of uplift force induced by the indenter can be approximated as a line load on the bottom surface of the floating plate, i.e.

$$\bar{q}(\bar{x}, t) = -\bar{P}(t)\delta(\bar{x}) \quad B. \tag{23}$$

For a given uplift motion, eqn (17a) can be reduced to a Volterra integral equation of the first kind:

$$w(0, \tau) = -\int_0^{\tau} P(u)[K(\tau - u)]\,\mathrm{d}u. \tag{24a}$$

where the kernel $K(b)$ is

$$K(b) = \frac{1}{\pi}\int_0^{\infty} \frac{\beta}{1+\sigma\gamma^2+\gamma^4}\sin(\beta b)\,\mathrm{d}\gamma. \tag{24b}$$

The Volterra integral equation (24a) is of the convolution type; a rigorous solution may be obtained by making use of the Faltung theorem for Laplace transforms (Sneddon, 1951). In the following, let $\mathscr{W}(0, s)$, $\mathscr{P}(s)$ and $\mathscr{K}(0, s)$ be the Laplace transforms of the functions $w(0, \tau)$, $P(\tau)$ and $K(0, \tau)$, respectively; eqn (24a) is then reduced to an algebraic equation,

$$\mathscr{W}(0, s) = -\mathscr{P}(s)\mathscr{K}(0, s), \tag{25}$$

where

$$\mathscr{W}(0, s) = -\int_0^{\infty} [\bar{l} - (1 - \mathrm{e}^{-\alpha\tau})\alpha]\mathrm{e}^{-s\tau}\,\mathrm{d}\tau = -\left[\frac{A}{s^2} - \frac{A}{s(s+\alpha A)}\right], \tag{26a}$$

$$\mathscr{K}(0, s) = \int_0^{\infty} \mathrm{e}^{-s\tau}\sin(\beta\tau)\,\mathrm{d}\tau \int_0^{\infty} \frac{\beta}{1+\sigma\gamma^2+\gamma^4}\,\mathrm{d}\gamma = \int_0^{\infty} \frac{1}{(s^2+\beta^2)\mu}\,\mathrm{d}\gamma, \tag{26b}$$

in which $A = (\rho_w - \rho_i)/(\rho g)$. The title problem is reduced to the problem of finding the inverse Laplace transform of $\mathscr{P}(s)$.

$$P(\tau) = \mathscr{L}^{-1}[\mathscr{P}(s)] = \mathscr{L}^{-1}\left[-\frac{\mathscr{W}(0, s)}{\mathscr{K}(0, s)}\right]. \tag{27}$$

The numerical technique of inversion of Laplace transforms described by Bellman *et al.* (1966) was initially used to evaluate the solution in eqn (27); the accuracy of the technique was assessed by numerically solving a number of convolution-type integral equations and found to vary considerably from equation to equation. An independent method of solution was therefore developed for comparative purposes. The latter method (described next) proved to be both more accurate and more reliable in the accuracy obtained. The results presented in this paper were obtained using the solution procedure now described.

Volterra integral equations of the first kind may sometimes be transformed into equations of the second kind (Baker, 1977), which can be readily solved; however, it is difficult to treat equations of the first kind directly. A solution $P(\tau)$ may not exist for every form of the forcing function that could be specified; when one does exist it may not be unique or it may be difficult to determine accurately (Baker, 1977). Ultimately, it proved advantageous to transform the integral equation (24a) into an integro-differential equation, viz.

Table 1. Characteristic length : ice thickness ratios

	Sea ice		Freshwater ice	
h(m)	l(m)	l/h	l(m)	l/h
0.05	1.27	25.4	1.90	38.1
0.10	21.3	21.3	3.20	32.0
0.50	7.14	14.3	10.7	21.4
1.00	12.0	12.0	18.0	18.0
3.00	27.4	9.13	41.0	13.7

$l = 12h^{3/4}$ (sea ice) and $18h^{3/4}$ (freshwater ice).

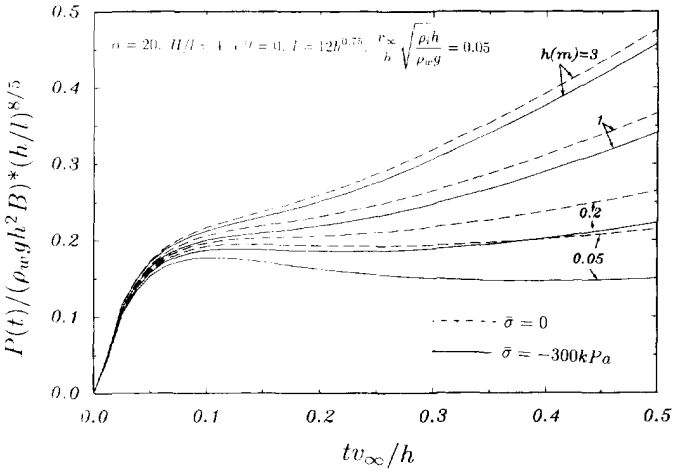

Fig. 7. Influence of in-plane stress on the uplift force for various sea ice thicknesses.

$$w(0,\tau) = -P(\tau)\bar{K}(0) + \int_0^\tau \frac{\partial P(u)}{\partial u}[\bar{K}(\tau-u)]\,\mathrm{d}u, \tag{28a}$$

where

$$\bar{K}(0) = (\sqrt{2})/4, \tag{28b}$$

and

$$\bar{K}(b) = \frac{1}{\pi}\int_0^\infty \frac{\cos(\beta_\gamma b)}{1+\sigma_\gamma^2+\gamma^4}\,\mathrm{d}\gamma. \tag{28c}$$

The ratio of characteristic length to plate thickness for sea ice is listed in Table 1. The influence of an in-plane stress on the uplift force for various sea ice thickness is shown in Fig. 7. The uplift force is normalized as $(\bar{P}(t)/\rho_w g h^2)\times(h/l)^{8/5}$ and the in-plane stress is assumed to be as low as -300 kPa. Obviously, for short times ($tv_\infty/h \leqslant 0.1$) the solutions with and without in-plane stress for various ice thicknesses nearly coincide. The influence of the in-plane stress on the uplift force is negligible for short times. However, for later times, the compressive in-plane stress reduces the uplift force significantly, especially for thinner ice sheets. Figure 8 shows the actual uplift force vs ice thickness for various times. The results reveal that the uplift force increases steadily with increasing ice thickness and rate of uplift.

The line loads required to uplift dynamically a floating plate according to the deflection–time uplift function specified in eqn (21) are plotted in Fig. 9 for various l/h ratios, and in Fig. 10 for various normalized uplift velocities $(v_\infty/h)\sqrt{(\rho_i h/\rho_w g)}$. In both plots, the ratio of the water depth to plate depth is a constant ($\bar{H}/h = 80$). The uplift load is plotted against non-dimensional time $\bar{t} = tv_\infty/h = \tau(v_\infty/h)\sqrt{(l/g)}$. Figure 9 reveals a significant

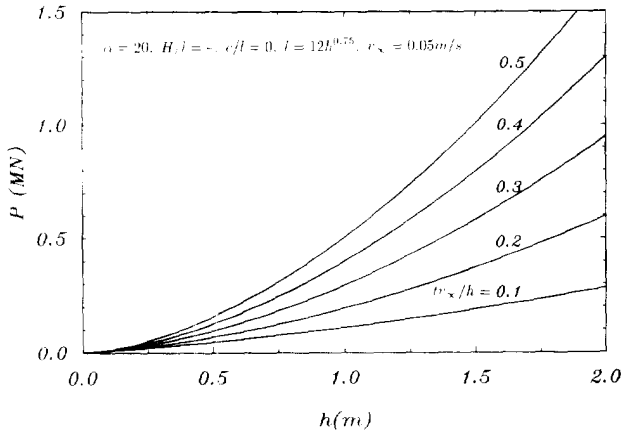

Fig. 8. Real uplift force vs sea ice thickness at various times.

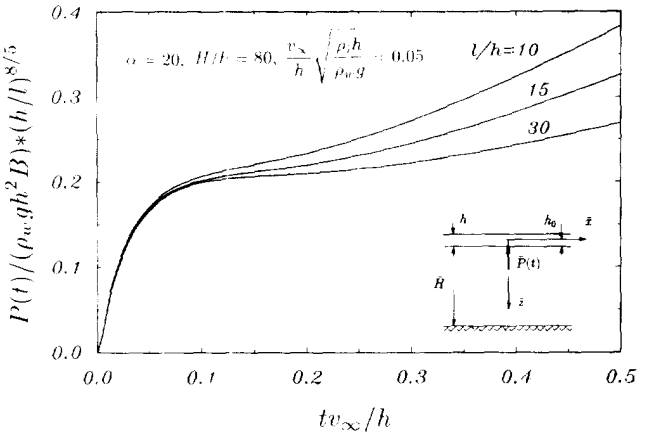

Fig. 9. Influence of the l/h ratio on the uplift force.

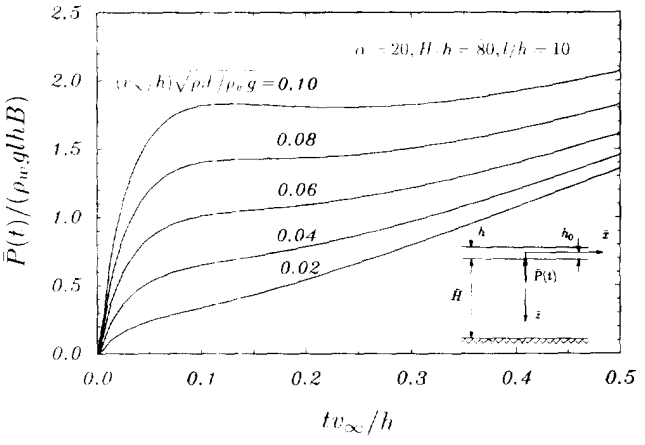

Fig. 10. Influence of the normalized indenter velocity v_∞ on the uplift force.

dependence on the characteristic length ratio l/h. However, if the uplift force is normalized as $(\bar{P}(t)/\rho_w g h^2) \times (h/l)^{8/5}$ all of the curves nearly coincide for early times ($tv_\infty/h \leqslant 0.2$). Note that the true uplift forces steadily increase as l/h increases, since a larger value of l/h—given a specific plate thickness h corresponds to a larger elastic modulus E'. An important feature of the uplift force is the very fast rate of increase for $tv_\infty/h \leqslant 0.1$; for later times, the rate of increase drops off substantially. The major component of the uplift force for early times is the inertia force imparted by the fluid that must be accelerated into motion by the plate. Figure 10 reveals that the uplift forces depends strongly on the eventual uplift

velocity v_s in eqn (21). It is worth noting that the magnitude of the uplift acceleration is given by $\alpha(v_s^2/h)e^{-v_s t/h}$. Larger values of v_s correspond to higher inertial forces and, consequently, higher uplift loads are expected during early times.

5. PLANAR VS AXISYMMETRIC

The response of a dynamically forced floating plate can readily be derived from the solution of an axisymmetric floating plate. The hydrodynamic solution of an infinite floating plate under a uniform distributed ring load (Dempsey and Zhao, 1993) is:

$$w(r,\tau)=\int_0^\infty \frac{\gamma\beta_\gamma}{1+\gamma^4}J_0(\gamma c)J_0(\gamma r)\,\mathrm{d}\gamma\int_0^\tau P(u)\sin[\beta_\gamma(\tau-u)]\,\mathrm{d}u, \tag{29}$$

where c is the radius of the ring and $P(\tau)$ is the non-dimensional load on the upper surface, and is defined as $P(\tau)=P'(\tau)/(2\pi\rho_w g l^2 h)$. For the concentrated load case, let $P(\tau)=P_0 f(\tau)$ and $c=0$; in this case eqn (29) is reduced to

$$w(r,\tau)=P_0\int_0^\infty \frac{\gamma\beta_\gamma}{1+\gamma^4}J_0(\gamma r)I(\beta_\gamma,\tau)\,\mathrm{d}\gamma, \tag{30}$$

where

$$I(\beta_\gamma,\tau)=\int_0^\tau f(u)\sin[\beta_\gamma(\tau-u)]\,\mathrm{d}u. \tag{31}$$

Since both the plate and the fluid foundation are linear, superposition can be employed for the solution under various loading combinations. Consider the load to be uniformly distributed in a straight line; the lateral concentrated load $P'(\tau)$ is now replaced by $P'(\tau)\,\mathrm{d}\eta'/B$ along a straight line, in which B is the range of the distributed load. The y coordinate coincides with the load line, while the x coordinate is normal to the load line. Should the dimension B be infinite, the solution should naturally be independent of coordinate y. The radius r in the Bessel function of eqn (30) represents the distance from the load point to the point of investigation, i.e. $r=\sqrt{(x^2+\eta^2)}$, in which η is the dummy argument in the y direction. Thus, the general expression for the displacement produced by a line load of finite length is

$$w(x,\tau)=\frac{P_0'}{2\pi\rho_w g B l^2 h}\int_{B/2}^{B/2}\mathrm{d}\eta'\int_0^\infty \frac{\gamma\beta_\gamma}{1+\gamma^4}J_0[\gamma\sqrt{(x^2+\eta^2)}]I(\beta_\gamma,\tau)\,\mathrm{d}\gamma. \tag{32}$$

Letting $B\to\infty$, $\eta=\eta'/l$ and remembering the identity (Erdelyi *et al.*, 1954)

$$\int_0^\infty J_0[\gamma\sqrt{(x^2+\eta^2)}]\,\mathrm{d}\eta=\frac{\cos(\gamma x)}{\gamma}, \tag{33}$$

eqn (32) quickly yields

$$w(x,\tau)=\frac{P_0'}{\pi\rho_w g B l h}\int_0^\infty \frac{\beta_\gamma}{1+\gamma^4}\cos(\gamma x)I(\beta_\gamma,\tau)\,\mathrm{d}\gamma. \tag{34}$$

Recalling the definition of the non-dimensional load P_0 in eqn (17a), eqn (34) is identical to the solution of a dynamically forced floating plate in the case of $c=0$ and $\sigma=0$.

6. CONCLUSIONS

The results from this study reveal that the effect of including the hydrodynamic reaction is significant. The fluid underneath the plate increases the mass and damping of the plate substantially. The added mass model does not have the potential to model the local dynamic response accurately since the required added mass coefficient is spatially and time dependent. Moreover, the global deformations are influenced greatly by the hydrodynamic coupling. The forced uplift study shows that the motion of the plate is dominated by the fluid inertia during the early stages of uplift.

Acknowledgement—This research was supported in part by the U.S. Office of Naval Research through its Sea Ice Mechanics Accelerated Research Initiative, grant Nos N00014-90-1360 and N00014-93-1-0714.

REFERENCES

Baker, T. H. C. (1977). *The Numerical Treatment of Integral Equations*. Oxford University Press, London.
Bellman, R., Kalaba, R. E. and Lockett, J. A. (1966). *Numerical Inversion of the Laplace Transform*. American Elsevier Publishing, New York.
Dempsey, J. P. and Zhao, Z. G. (1993). Elastohydrodynamic response of an ice sheet to forced sub-surface uplift. *J. Mech. Phys. Solids* **41**, 487–506.
Dempsey, J. P., Zhao, Z. G., Minnetyan, L. and Li, H. (1990). Plane contact on an elastic layer supported by a Winkler foundation. *J. Appl. Mech.* **57**, 974–980.
Erdelyi, A., Magnus, W., Oberhettinger, F. and Tricomi, F. G. (1954). *Tables of Integral Transforms*, Vol. II. McGraw-Hill, New York.
Kheisin, D. Y. (1967). Dynamics of the ice cover. *Gigrometeorolicheskoe, Izdat-el'stvo, Leningrad* (U. S. Technical Translation FSTC-HT-458-69).
Nevel, D. (1970). Vibration of a floating ice sheet. CRREL Research Report 281, Hanover, New Hampshire.
Sodhi, D. S. (1989). Interaction forces during vertical penetration of floating ice sheets with cylindrical indentors. *Proceedings of the 8th International OMAE Conference*, Vol. IV, pp. 377–382.
Sneddon, I. N. (1951). *Fourier Transforms*. McGraw-Hill, New York.
Timoshenko, S. (1958). *Strength of Materials, Part II*. Van Nostrand, New York.